CEBAF Program Advisory Committee Nine
Extension and Update Cover Sheet

This update must be received by close of business on Thursday, December 1, 1994 at:

CEBAF

User Liaison Office, Mail Stop 12 B

12000 Jefferson Avenue

Newport News, VA 23606

Experiment: E 94 - 016

Check Applicable Boxes:

☐ Extension ☐ Update ☑ Hall B Update

Contact Person

Name: Alex R. Dzierba

Institution: Indiana University

Address: Dept. of Physics

Address:

City, State ZIP/Country: Bloomington, IN 47405/USA

Phone: 812/855-9421 (office)
812/825-4063 (home)

FAX: 812/855-0440 (office)
812/825-4152 (home)

E-Mail → Internet: dzierba@ind.physics.indiana.edu

CEBAF Use Only

Receipt Date: 12/15/94

By: gp

PR 94-134

Section 1 - Introduction

This is an update to PR-94-016, a proposal to measure rare radiative decays of the ϕ meson to study the structure of daughter states as well as to probe symmetry violations.

In this update we do not review the physics goals of the experiment.
We refer to the original proposal for a detailed discussion of the physics goals.

This update focuses on the issue of whether hadronic processes and electromagnetic backgrounds in Hall B could present a problem in achieving the required sensitivities. Section 2 describes the detailed Monte Carlo studies recently performed to address these issues. The conclusion is that these backgrounds do not present a problem.

Section 3 summarizes some recent experimental issues including (1) a possible beam pipe to reduce backgrounds; (2) the charged particle veto wall design; (3) a description of a first-level trigger and tests; (4) a proposed overall trigger scheme; (5) the integration with the Hall B data acquisition system; (6) R & D on the high-voltage system; (7) a calibration technique and (8) the plans for the detector housing.

In summary, the physics motivation remains as strong as ever. Monte Carlo studies as well as recent progress on analysis of real data from an AGS experiment at BNL reassure us that we will meet our goals. Progress is being made on various experimental fronts (hardware and software) as well.

Section 2 - Monte Carlo Background Studies

2.1 Introduction

The issue is whether or not we will be able to measure the relevant branching ratios of the ϕ meson at the required sensitivity in the presence of known hadronic backgrounds and in the presence of electromagnetic backgrounds which can be expected in the tagged photon beam in Hall B. In order to answer this question we have simulated the response of the detector to photons produced from (1) the signal events (radiative ϕ decays); (2) hadronic processes (yielding photons from multiple π^o and η mesons); and (3) electromagnetic background processes expected in the Hall B tagged photon environment. A sample of such events were generated (physics plus random backgrounds) and the lead glass detector (LGD) analysis code from Brookhaven AGS Experiment E852 was used to extract the signal. Our conclusion from these studies is that the hadronic and electromagnetic backgrounds do not prevent us from measuring the signal decays at the required sensitivity.

2.2 Modeling the LGD Response

The most compute-intensive part of this Monte-Carlo simulation is the estimation of a simulated LGD signal due to a photon striking the lead glass array. Existing software packages (for example GEANT) are capable of generating a simulation of the production, subsequent decay and energy deposition in lead glass of arbitrary classes of events. Since the purpose of the study is to determine if rare signals can be observed in the presence of far more copious backgrounds it is required that large numbers of complicated background events be generated. This requires that an alternative and highly efficient detector simulation method be employed.

GEANT was used to generate photon energy deposition maps for a large number of photons. These maps were stored in a look-up table and used by another program that generated photon 4-vectors as specified by a either a hadronic production mechanism and a subsequent decay tree or random electromagnetic processes.

The photon energy maps stored in the look-up tables were generated by using GEANT to generate one photon per square centimeter in the detector. Each square centimeter was illuminated by *60* photons between *0.1 GeV* and *6 GeV*. GEANT was used to generate the electromagnetic showers due to these photons and the total path length of the electrons and positrons from this shower was calculated for each block in the array.

These lengths were then multiplied by a numerical factor to allow us to interpret them as energy depositions. This method simulates the mechanism that generates the signals in a lead glass calorimeter. The amount of Cerenkov light *produced per centimeter of electron/positron path length* is a constant, provided that $\beta \approx 1$. This simulation technique is indeed highly efficient and has been used extensively in BNL E852 where it correctly simulates the detector response for well known hadronic processes with multiple combinations of π^o and η mesons.

2.3 *Hadronic Processes*

Assuming a $1/E_\gamma$ spectrum for photons, $E_\gamma^{max} = 6\ GeV$ and $5 \times 10^7\ photons/sec$ in the range $4.5 < E_\gamma < 6.0\ GeV$, the total hadronic production rate is $\approx 150\ KHz$. In this experiment we will trigger only on events with no charged forward particles into the LGD. The hadronic rate for processes yielding only photons in the forward direction is $\leq 100\ KHz$ and is dominated by $\gamma n \rightarrow \pi^o n$ and $\gamma p \rightarrow \pi^o p$ which accounts for $\approx 75\ KHz$. Since we have an effective mass trigger processor (which has been demonstrated to work in BNL E852) we expect to reject the great majority of single π^o events in the trigger. Our off-line mass resolution of $\sigma = 10\ MeV$ at the π^o mass is more that adequate to reject this background.

The major contributor to other hadronic processes yielding forward photons are the production of the vector mesons: ρ, ω and ϕ. The photoproduction cross sections are in the ratio:

$$\sigma(\gamma p \rightarrow \rho p) : \sigma(\gamma p \rightarrow \rho p) : \sigma(\gamma p \rightarrow \rho p) \approx 36 : 4 : 1$$

This ratio, convolved with the fraction of ρ, ω and ϕ decays into all photons, yields the following: $N(\rho \rightarrow photons) : N(\omega \rightarrow photons) : N(\phi \rightarrow photons) \approx 3.8 : 34 : 1$.

Since our trigger will require that the energy deposited in the detector be a large fraction of the tagged photon energy, the trigger rate will be dominated by neutral decays of vector mesons other than the ϕ. Table 1 gives the expected number of neutral events produced. The unknown branching ratios for $\phi \rightarrow f_o\gamma$ and $\phi \rightarrow a_o\gamma$ were chosen so that *2000* events would be generated by the Monte-Carlo program. The photon 4-vectors were generated using conservation of energy and momentum in a sequential decay tree. The angular distributions used to populate the decay phase space took into account the polarization of the initial state vector mesons. Flat angular distributions were used for the spinless daughters of the primary meson. The 4-vector of the primary meson was calculated assuming an incident photon beam illuminating a $1 \times 1 \times 1\ cm^3$ target. The momentum-transfer-squared (t) from incident photon to outgoing meson was required to follow the distribution: $\frac{dN}{d|t|} \propto e^{-4|t|}$. The fraction satisfying the trigger was calculated by requiring more than 5.5 GeV (from a 6 GeV photon beam) be deposited in the detector.

2.4 *Random Electromagnetic Background*

In addition to the backgrounds discussed above, we have considered backgrounds associated with random photon interactions occuring in coincidence (or nearly so) with interesting events. The expected rate for these random coincedences was calculated as follows:

- 10^7 beam photons were generated with a bremhstrulung momentum distribution
- these photons were tracked through the materials expected to be encountered by the beam
- GEANT was used to simulate the interactions of these photons

It was determined that 5×10^5 or *5 %* of these photons interacted and produced one or more secondary

particles that struck the active area of the detector. The total photon beam rate was normalized such that the tagged rate for photons between 4.5 and 6.0 GeV was 5×10^7. The incident photon momentum spectrum was integrated between 0.075 and 6.0 GeV to obtain a total beam photon rate of $7.6 \times 10^8 / sec$. We do not consider photons with energy lower than 75 MeV since it is unlikely that we will configure the analysis algorithms to be sensitive to photons with energy significantly smaller than ≈ 150 MeV. The number of interactions (yeilding energy deposition in the detector) per trigger is then determined as the product of the total beam rate, the fraction of this yeilding energy deposition in the glass and the length of the event gate. We anticipate using a gate of 250 nanoseconds so the random event rate is then 9.5 per trigger. To simulate this effect, we chose a random number from a poisson distribution with a mean of 9.5 and superimposed this number of random events on interesting events generated as above. The energy deposited in each block of the array was determined with the methods described above.

2.5 *Analysis Method*

The analysis proceeds in three steps:

- Reconstruction of the photon 4-vectors from the energies deposited in the detector
- Assigning photons to massive parents and evaluating effective mass distributions of various combinations photons and massive parent particles
- Extraction of branching ratios of the ϕ from these effective mass distributions

Photons deposit energy in several blocks. The first step in reconstruction of the photon 4-vectors is the pattern recognition problem of determining the impact point and energy of the photons from these clusters. The algorithms for this have been developed for BNL E852 and extensively tested on data from that experiment. Once these parameters are known, the vector part is determined geometrically by assuming the photon originated in the center of the target.

The photons are assigned to massive parents by evaluating the χ^2 of the relevant hypotheses for all combinations of photon assignments. Ambiguities are resolved with *a priori* knowledge of the relative probabilites of the final state topologies assumed in the hypothesis testing.

2.6 *Analysis Method Applied to BNL E852*

One of the best tests of the analysis technique is to see it applied to real data. Figs 2.1 through 2.6 show mass spectra from multi-photon final states produced in $\pi^- p$ interactions 18 GeV from a sample of 1.7M triggers. In Fig 2.1, the $\omega \to \pi^\circ\gamma$ is observed in the 3-photon sample. In Figs 2.2 and 2.3, distributions from the 4-photon sample are shown. The $K_S^\circ \to \pi^\circ\pi^\circ$, $f_2(1275) \to \pi^\circ\pi^\circ$, $a_0(980) \to \pi^\circ\eta$ and $a_2(1320) \to \pi^\circ\eta$ are observed. Fig 2.4 shows the $\pi^\circ\gamma$ mass spectrum from 5-photon events which reconstruct to $\pi^\circ\pi^\circ\gamma$. The radiative $\omega \to \pi^\circ\gamma$ decay is observed in this complicated topology. Finally, in the 6-photon sample (Figs 2.5 and 2.6) the $\eta \to \pi^\circ\pi^\circ\pi^\circ$, $\eta' \to \eta\pi^\circ\pi^\circ$ and $f_1(1280) \to \eta\pi^\circ\pi^\circ$ decays are observed. Since one of the goals of this Hall B experiment is to measure the decays $\phi \to f_0\gamma$ and $\phi \to a_0\gamma$, it is interesting to note that the a_0 is clearly seen in Fig 2.3 and the f_0 manifests itself as a dip at about 1.0 GeV in the plot of Fig 2.2. This effect has been seen in other experiments and is due to the $\pi^\circ\pi^\circ$ phase shift going through 180° at the f_0. In summary, the examples of Figs 2.1 through 2.6 illustrate that:

- Techniques to analyze multi-photon events exist and have been extensively tested with data
- Different decay chains can be reconstructed from events with identical photon multiplicity
- Signals can be extracted from events occurring at the level of $\approx 10^{-4}$

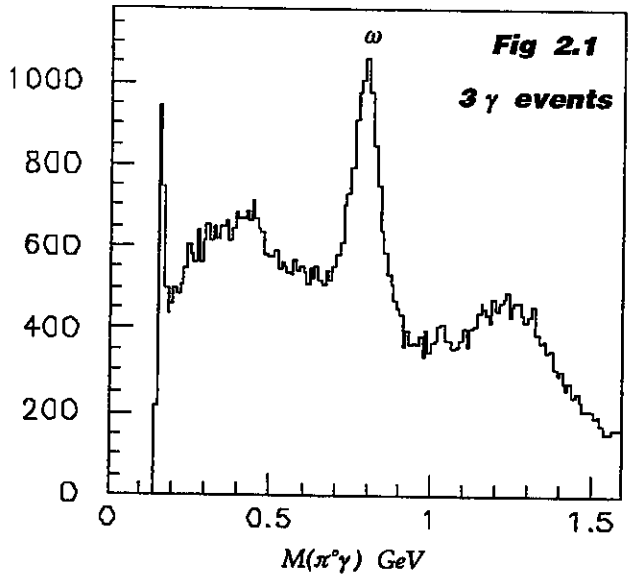
ω
Fig 2.1
3 γ events
1000
800
600
400
200
0
0
0.5
1
1.5
M(π°γ) GeV

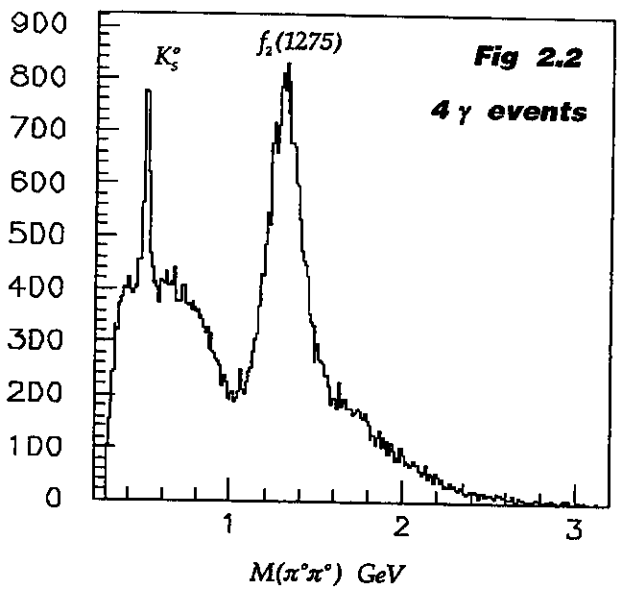
K°s
f2(1275)
Fig 2.2
4 γ events
900
800
700
600
500
400
300
200
100
0
1
2
3
M(π°π°) GeV

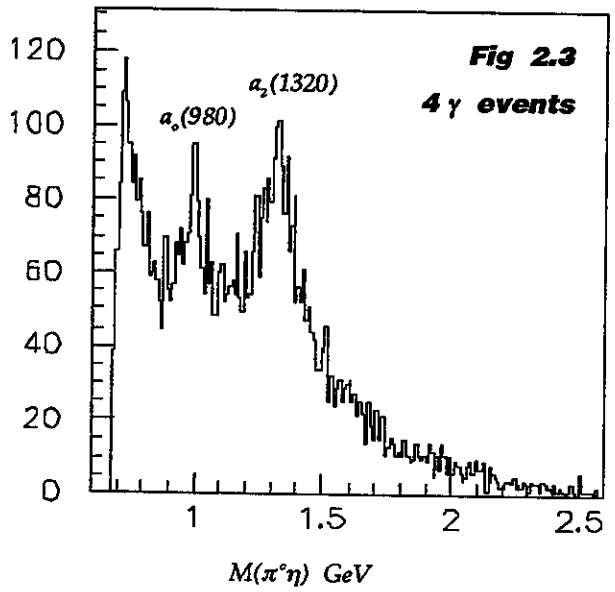
a0(980)
a2(1320)
Fig 2.3
4 γ events
120
100
80
60
40
20
0
1
1.5
2
2.5
M(π°η) GeV

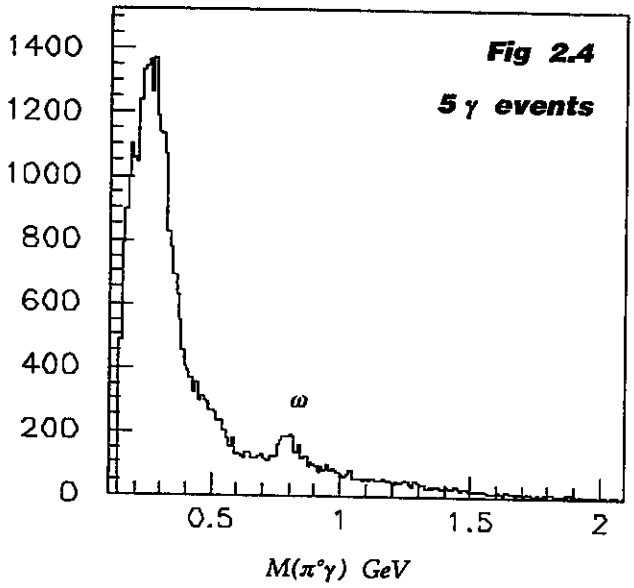
ω
Fig 2.4
5 γ events
1400
1200
1000
800
600
400
200
0
0.5
1
1.5
2
M(π°γ) GeV

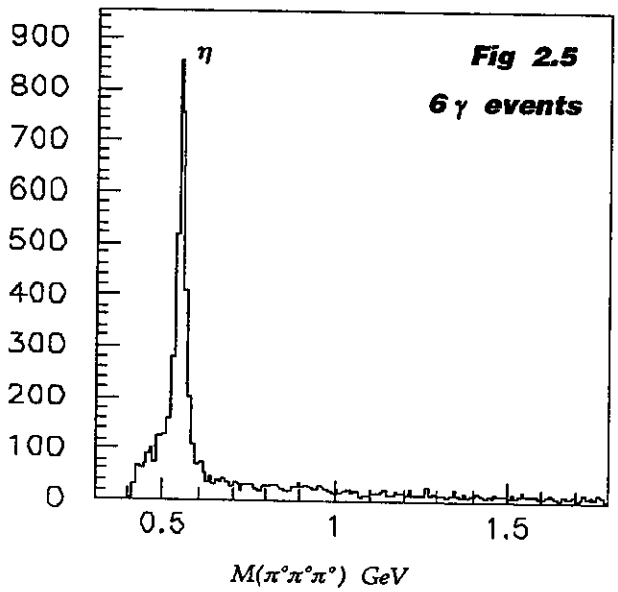
η
Fig 2.5
6 γ events
900
800
700
600
500
400
300
200
100
0
0.5
1
1.5
M(π°π°π°) GeV

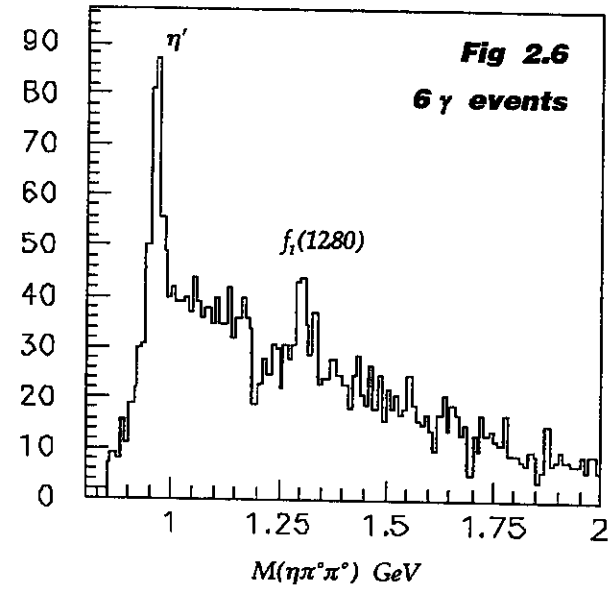
η'
f1(1280)
Fig 2.6
6 γ events
90
80
70
60
50
40
30
20
10
0
1
1.25
1.5
1.75
2
Mηπ°π°) GeV

2.7 Analysis of the Monte Carlo Events

Because of the large numbers of ω and ρ decays, the analysis required that the photon system have a total effective mass within *60 MeV* of the ϕ mass. ($\approx 2\sigma$ of the $\phi \to \eta\gamma$ Monte-Carlo effective mass distribution) Decay modes of the ϕ are then identified by the presence of resonances in the effective mass distributions of the daughter particles of the supposed ϕ. For example, Fig. 2.7 shows the $\pi^\circ\pi^\circ$ effective mass from $\pi^\circ\pi^\circ\gamma$ events and Fig. 2.8 shows the $\pi^\circ\eta$ effective mass from $\pi^\circ\eta\gamma$ events. The fitted functions superposed on these figures are the shapes expected from $\phi \to f_o\gamma$ and $\phi \to a_o\gamma$. .These functions were generated by fitting the effective mass distributions obtained from a Monte-Carlo that generated *only* $\phi \to f_o\gamma$ or $\phi \to a_o\gamma$ events. There is a single parameter in each of these functions that is interpreted as the number of events produced. All acceptance corrections and combinatoric effects are included in these functions. Since 2000 Monte-Carlo events were generated for each of these modes it is expected that 2000 events be observed after acceptance corrections. The result is there were 1500 ± 150 events due to $\phi \to f_o\gamma$ and 2130 ± 185 events due to $\phi \to a_o\gamma$. The overall result is that the geometrical acceptance convoluted with reconstruction efficiency in sorting out the signal from the sea of background events is of order 10 % for these decays.

Work is in progress in understanding the effect of adding random noise from electromagnetic backgrounds to the Monte Carlo signal events. Since we add an average of 9.5 random noise events per trigger, we have been able to analyze only 10 % of the Monte Carlo sample at this writing. The preliminary result from the analysis of the $\phi \to f_o\gamma$ and $\phi \to a_o\gamma$. decays is that the electromagnetic noise is not a problem. The random noise does not effect the ability to reconstruct the $\phi \to \pi^\circ\gamma$ and $\phi \to \eta\gamma$ decays as can be seen in Figs. 2.9 and 2.10.

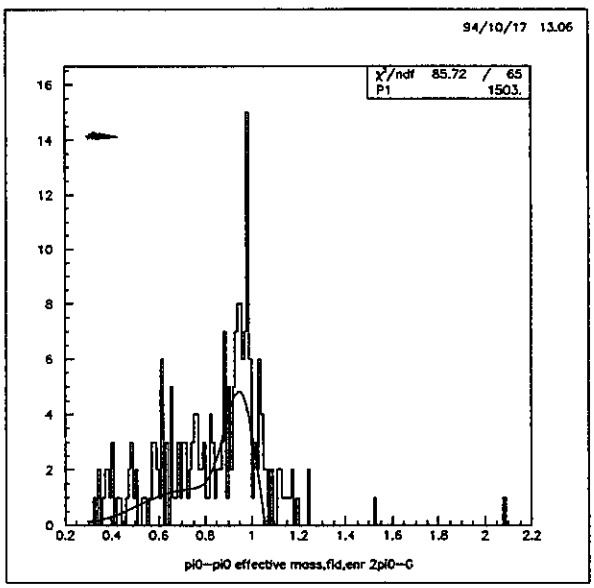

Fig 2.7: *The $\pi^\circ\pi^\circ$ effective mass spectrum showing the $f_o(975)$ signal. The observed signal corresponds to a generated branching ratio of 2.1×10^{-4}, which is the current limit.* ***In the requested running time we would expected to se a yield a factor of 75 higher compared to what is presented in this plot.***

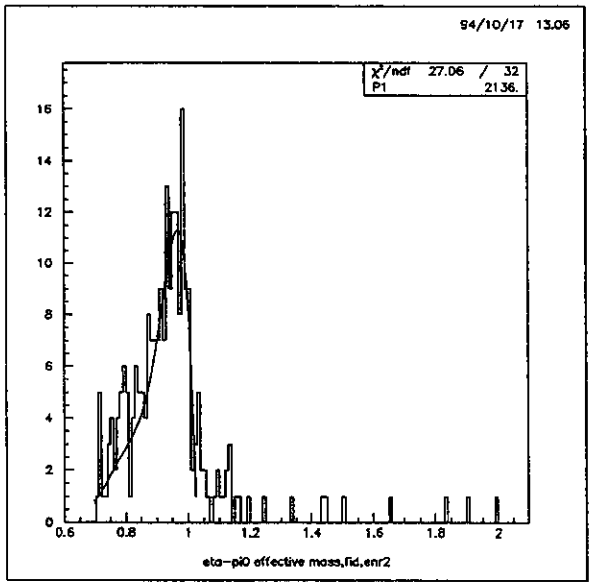

Fig 2.8: *The $\pi^\circ\eta$ effective mass spectrum showing the $a_o(980)$ signal. The observed signal corresponds to a generated branching ratio of 5.2×10^{-4}, which is the current limit.* ***In the requested running time we would expected to se a yield a factor of 30 higher compared to what is presented in this plot.***

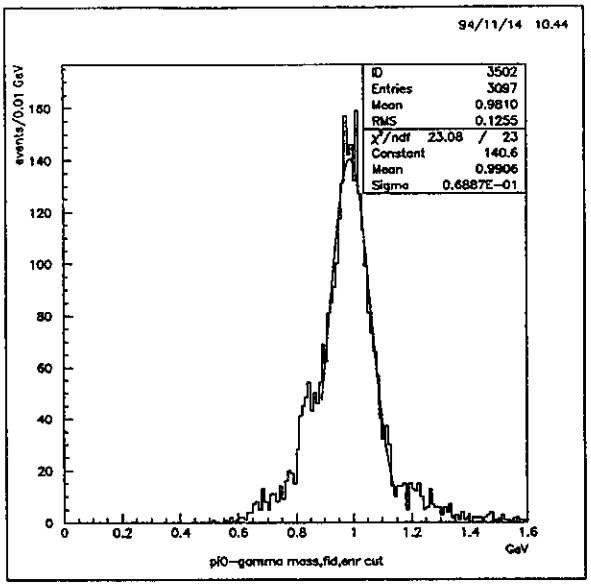

Fig 2.9: *The $\pi^0\gamma$ effective mass spectrum from $\phi \rightarrow \pi^0\gamma$ Monte Carlo events generated with an average of 9.5 random noise events per trigger.*

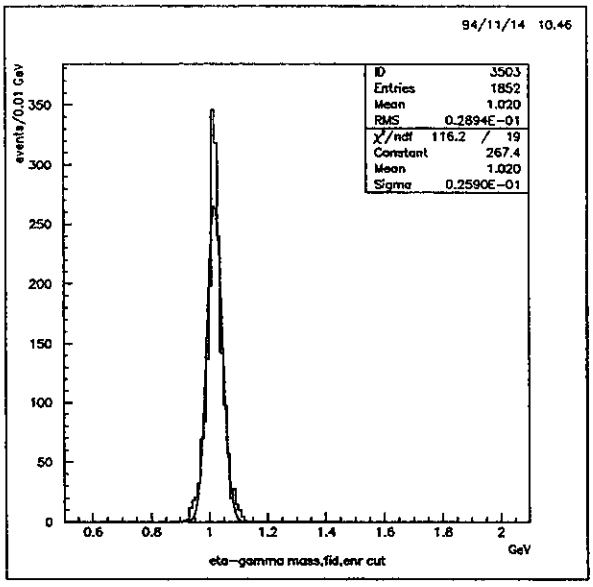

Fig 2.10: *The $\eta\gamma$ effective mass spectrum from $\phi \rightarrow \eta\gamma$ Monte Carlo events generated with an average of 9.5 random noise events per trigger.*

Section 3 - Experimental Issues

3.1 Beam Pipe

To reduce interactions of the primary beam that could limit the detector's sensitivity we are studying the possibility of installing a Be beam pipe downstream of the target to at least the back end of the calorimeter. This pipe should be made of Be to reduce conversions. This vacuum pipe would be linked to one of more conventional material downstream of the calorimeter to propagate the remains of the photon beam to a dump.

3.2 Veto Wall

The charged-particle veto counter will consist of 24 pieces of Pilot U or NE102A plastic scintillator; a single phototube will view each piece of scintillator from one end, and the phototube base will be optimized for fast timing. The layout shown in Fig. 3.1 was designed on the basis of the criteria that the count rates in the scintillators should be as well-matched as practical, and that the rate not exceed approximately *1 MHz* in any piece. The rates for this design procedure were obtained from Monte-Carlo estimates of the charged-particle background in the experiment at an incident bremstraahlung flux *useful* flux of 5×10^7 *photons/sec* between *4.5* and *6 GeV*. Only the electromagnetic rate was considered since the hadronic background is negligibly small. The calculated rates for each of the pieces under these conditions is given in Fig. 3.1; it can be seen that the design criteria are met. The thickness of the scintillator pieces shown in Fig. 3.1 will be *4mm*, based on considerations of structural stability and sufficient light output for minimum ionizing particles to ensure efficient charged-particle rejection. The edges of each piece will suffer from light-collection problems, so the pieces will overlap by some amount at their edges. In addition, some consideration is being giving to duplicating the central pieces and overlapping them fully to further increase the rejection probability.

3.3 First Level Trigger

The first level trigger we intend to use is based on a set of thin wave-shifting plastic strips located behind the lead glass blocks. These strips are excited by the Cerenkov radiation produced by showers in the lead glass

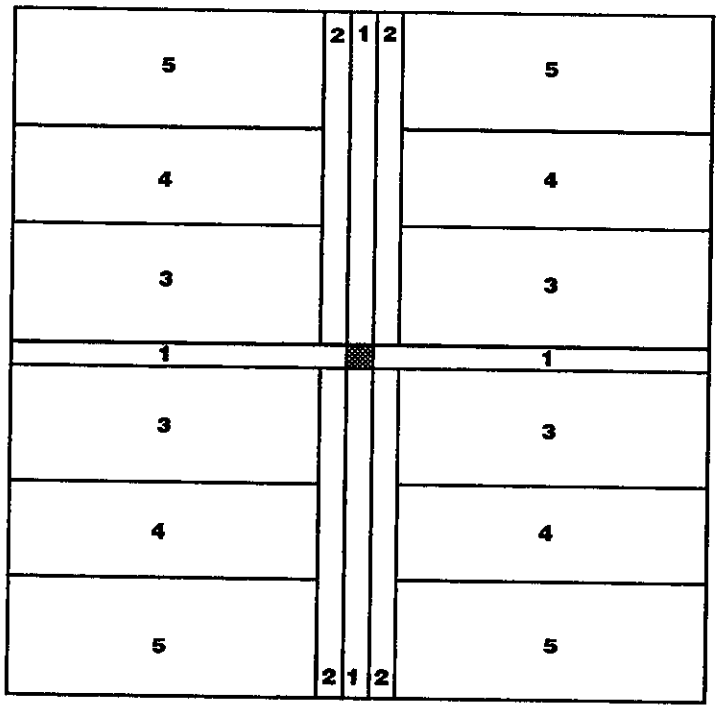

Fig 3.1: *Charged particle veto wall segmentation. The estimated rates per element are:*

1: 8.9×10^5 / sec
2: 5.4×10^5 / sec
3: 7.3×10^5 / sec
4: 2.6×10^5 / sec
5: 1.0×10^5 / sec

blocks but are insensitive to charged particles, giving us the ability to select events with electromagnetic interactions in the array. This pre-trigger will consist of 25 *0.25-in* type NE 174 wave-length shifting plastic strips. These strips will be located between the phototubes used for the readout of the array and immediately behind the back face of the lead glass blocks. These strips exit the sides of the light tight enclosure holding the readout phototubes and are ganged together to illuminate several RCA8575 phototubes. The output of these tubes is discriminated and logical functions of these signals is used to determine the pre-trigger state. We have tested this idea with a small prototype $(5 \times 5$ *blocks*$)$ detector using cosmic ray muons as the signal source. While these muons do not generate electromagnetic showers in lead glass, they do generate Cerenkov light. In the test setup the signals are small but discernible and have given us confidence that the system is workable.

3.4 Overall Trigger

The trigger system relies on a simple fast trigger to strobe the lead glass ADC units and a second level trigger based on a trigger processor to analyze the data from the lead glass and makes a decision in about *1.0* μs after the ADCs finish their *4.0* μs acquisition and conversion cycle.

The total particle flux hitting the lead glass is expected to be on the order of *50 MHz* but the ADCs cannot handle data faster than about *0.5 MHz*. The fast trigger selects the good events and identifies them to the ADC system. The three possible components of the fast trigger in order of usefulness are the signals from the lead glass array (described above), the signals from the photon tagger and the signals from the veto counters.

In case the lead glass signals alone do not provide a trigger which is restrictive enough, the other sources of trigger information can be used.

The signals from the photon tagger run at the full tagged photon rate of nominally *50 MHz*. We would share the electronics that is being set up for the CLAS experiment where signals from all the timing counters are combined by a master OR circuit. The resulting signal has better timing properties than the signals from the wave shifter bars. The random rate, from tube noise or neutron interactions, and the rate from untagged photons would be reduced by about a factor of 5 by using the tagger signal. The difficulty is that there is a

longer delay in this signal. A convenient way of using this signal is therefore to exploit the fast clear capability of the ADCs. The ADCs would be strobed as above at rates up to *0.5 MHz*. A coincidence of the strobe with the tagger signal would veto a fast clear which would otherwise occur about *300 ns* after the strobe.

The veto counters are important for identifying electrons and other charged particles which hit the lead glass. Putting them in the trigger would reduce the trigger rate by removing electron triggers and also minimum ionizing charged particles that produce a large enough pulse height in the lead glass to simulate electrons. These counters would however only be used if absolutely necessary. Poor performance of these counters could cause unknown losses of events, and the high rate would accidentally veto good events. If used in the trigger, the signals from the separate sections of the veto counters would veto signals from corresponding sections of the lead glass array to reduce accidental vetos. The signals from the different sections would then be combined to form the ADC strobe.

The second level trigger employs a trigger processor similar to the one used in experiment E-852 at the AGS at Brookhaven National Laboratory. It analyzes the data from the lead glass and calculates approximately the total energy, the multiplicity, the invariant mass and the square of the momentum-transfer. Triggers can be accepted or rejected based on the results of these calculations. This is a very powerful method for rejecting unwanted events before they are transferred to the data acquisition system. Typically it can be set to accept only high mass states. We expect that the final trigger rate will be within a factor of two of the true physics rate.

Fig 3.2 shows a trigger logic diagram which is somewhat conceptual but also has considerable detail. The PMSIGNAL from the wave shifter bars goes to a discriminator which generates the ADCGATE. A coincidence between the TAGGER and the discriminated PMSIGNAL causes the tagger and veto TDCs to be strobed and the lead glass data to be processed in the trigger processor, whereas, no coincidence causes the ADCs to be cleared. A busy line holds off any further gates until current activity is completed.

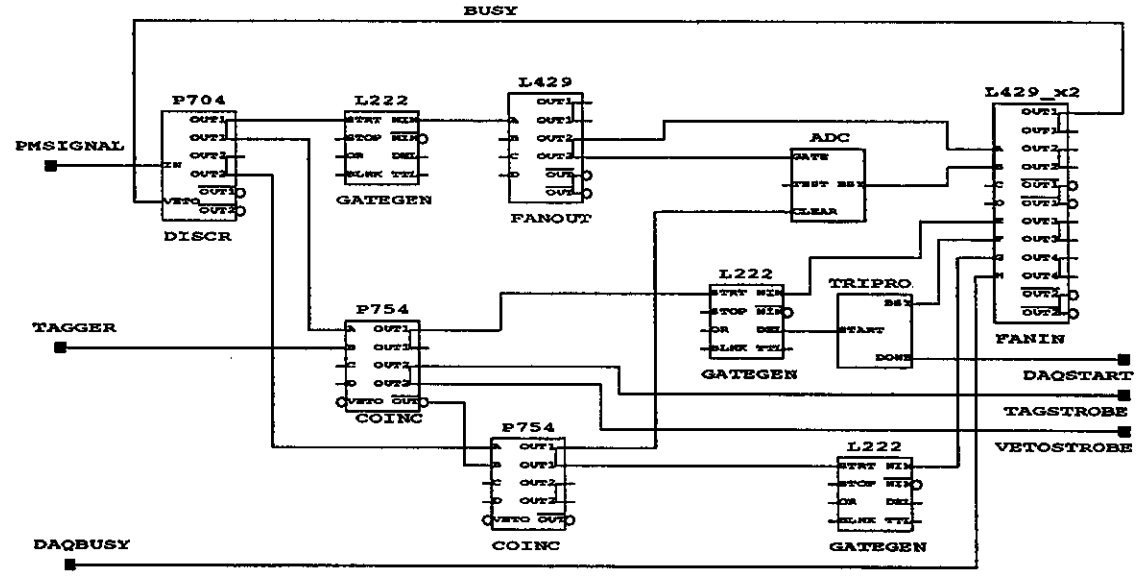

TRIGGER CONCEPT

Fig 3.2: *Tentative trigger design*

3.5 Integration of the LGD with CEBAF Hall B DAQ

Hall B has adopted the EPICS (Experimental Physics and Industrial Control System) system for its slow controls. This system appears to have all of the capabilities that we will need to (1) set voltages, (2) read out voltages periodically, (3) insert periodic monitoring (laser) events into the data stream, and (4) read out other monitoring systems, such as temperature and humidity.

A robust DAQ system is currently being developed for CEBAF called CODA (CEBAF On-line Data Acquisition) which will be used by Hall B, and by this experiment as well. The Hall B Collaboration is working with the Controls Group to integrate EPICS and CODA, and there is no reason to move to a custom DAQ system, since the needs of this experiment fall well within the capabilities of CODA.

The need for access to data on-line for analysis is very important for the calibration of the LGD, and for the smooth running of the experiment. There is a mechanism in place for sampling data for the CODA data stream, and this will be more than adequate for our needs.

The CLAS detector will generate an immense amount of data (up to *20MB/sec*). This large data rate requires special tape handling facilities, with very fast, very expensive, high capacity tape drives. This experiment will only generate a fraction of that data rate, on the order of *1MB/sec*. Thus the CLAS tape writing system is overkill, and in fact may impede the analysis of data since the raw tapes will not be in a format that most institutions can use. Either a program to immediately transfer data from CLAS tapes to a lower capacity standard (DAT, 8mm, DLC, etc.) is needed, or the data needs to be written to the lower capacity drives initially. Which system is preferable is not clear at this time.

3.6 High Voltage System R & D

A Cockcroft-Walton voltage multiplier is in use in BNL E852 to power the Russian FEU 84-3 phototubes. This system dissipates far less power than the usual resistor divider string and also eliminates the need for an extra high-voltage cable for each channel. Our experience with the system now in use led us to propose a number of improvements. An R&D program is underway before building the 625 bases needed for this experiment.

The operating voltage is set digitally over a serial data bus. The base will also include a pulser which has an amplitude proportional to the high voltage setting as a read back mechanism. The system under design provides a maximum photocathode voltage of *2047 volts* and a maximum anode current of *150 μamps*, has a minimum power consumption (at idle) of *50 mW* and a maximum power consumption of *150 mW* and has an input voltage of 14 to 18 volts.

3.7 Calibration Technique

We intend to calibrate the lead glass array with electron-positron pairs produced by tagged photons incident on a thin radiator positioned ≈ 8 *m* upstream of the front face of the detector. Since the angle of these particles (to the photon beam) is very small we will require a magnet to obtain a complete illumination of the detector. We discuss below the assumptions that lead to a specification of the magnet we will need.

We assume that the radiator will be located as close as possible to the photon exit flange of the tagger. (this location is inside the alcove containing the tagger) We also assume that the calibration magnet will not be supported by the floor of the Level 1 platform but will be supported by an independent stand upstream of the most upstream limit of Level 1. We take the center of the magnetic aperture to be four feet upstream of the upstream limit of Level 1. We take the front face of the detector to be located *10 ft.* upstream of the downstream limit of the Level 1 platform. This determines the magnet center to lead glass face distance as *24 ft.*

To calibrate the detector we must illuminate it with electrons (positrons) with an energy approximating the typical photon energy we will encounter in our experiment. We take this energy to be *1 GeV*. Since we must illuminate the entire detector, the largest distance from the beam centerline to which electrons must be

transported is the distance from the detector center to a detector corner or *71 cm*. This implies the bend angle for *1 GeV* particles is *96.8 mr*. Since

$$\sin\theta = \frac{0.3 \cdot B \cdot \ell}{p}$$

(with B in Tesla, ℓ in meters and p in GeV/c) and $p \approx 1\ GeV$, the field integral is determined to be *0.322 Tesla-meters*. We point out that this is the mimimum required field integral.

We must be able to rotate this magnet through *180°* to fully illuminate the detector. We request a computer controllable rotating fixture to accomplish this. We also request the magnet and an appropriate computer controllable power supply.

3.8 The Detector Housing

A schematic of the detector is shown in Fig. 3.3. The outside dimensions are 120 in (long) by 96 in (wide) by 115 in (high). The center of the glass stack is about 7 ft from the floor. A darkroom area (accessed via a revolving door) will allow one person at a time to work on the glass wall and phototubes in a humidity and temperature controlled environment. The box will be lifted at the corners. Reinforcing rods will run down the coner structural tubes and attach under the platform frame. This will maintain as much of the load in compression as possible while relieving unecessary stress from the welded frame holding the glass. The glass stack will weigh about 3800 pounds while the entire detector will weigh not exceed 12,000 pounds. We anticipate using the rails for the CLAS Region 1 insertion fixture to move our detector into position.

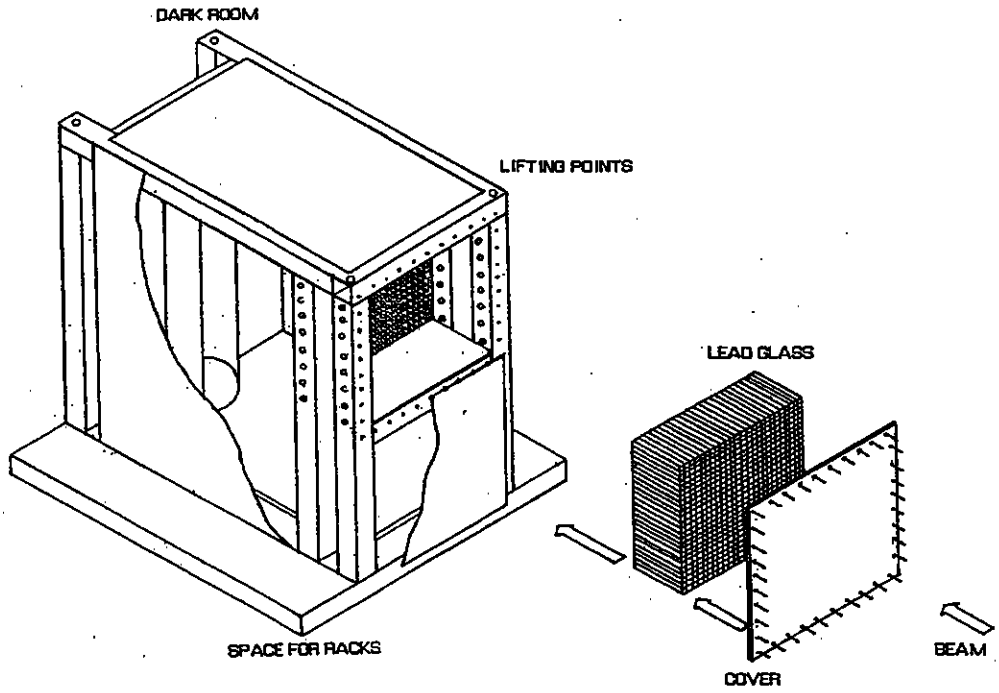

Fig. 3.3: *LGD Housing*

Continuous Electron Beam Accelerator Facility
12000 Jefferson Avenue
Newport News, Virginia 23606
(804) 249-7426
Fax: (804) 249-7398
Internet: Grunder@CEBAF.GOV

DIRECTOR'S OFFICE

December 9, 1994

Dr. A. R. Dzierba
Department of Physics
Indiana University
Bloomington, IN 47405

Dear Dr. Dzierba:

Your proposal, "Measurement of Rare Radiative Decays of the ϕ Meson", PR94-016, was recommended for conditional approval in Hall B by the CEBAF Program Advisory Committee (PAC). I have accepted the PAC's recommendation and would like to encourage you to continue to use CEBAF and its User community as resources to support you on your proposal so that it will be in a position to go before a future PAC for consideration for full approval. The full report of the PAC, including the discussion of your proposal, was mailed to you in August.

Experimental equipment construction proceeds on schedule in Halls A and B and operations have begun in Hall C. It is important that you and your proposal collaboration work closely with Bernhard Mecking and Larry Dennis and the Hall B Collaboration in preparing the experimental program and equipment. We want to be certain that the facilities are optimally prepared to begin performing experiments.

I would like to thank you for dedicating so much effort to the CEBAF research program and look forward to working with you.

Sincerely,

Hermann A. Grunder
Director

cc: J. Napolitano